

# EVIDENCE FOR HAIRPIN PACKET STRUCTURE IN DNS CHANNEL FLOW

Zi-Chao Liu  
Ronald J. Adrian

Department of Theoretical and Applied Mechanics  
University of Illinois at Urbana-Champaign  
Urbana, IL 6801, USA

## ABSTRACT

Experimental studies of boundary layers and channel flows with 2-D PIV measurements have revealed that wall turbulence is thickly populated with hairpin vortices that mostly appear in groups as “packets”. A recent numerical simulation study of the evolution of a single hairpin-like vortex has disclosed the mechanism for the generation of near-wall hairpin vortex packets. However, there are very few observations of hairpins in existing DNS studies, and none have revealed packets. The present study demonstrates, for the first time, the existence of hairpin vortex packets in DNS of turbulent flow. Vortex packets are found to appear frequently in DNS of fully developed turbulent channel flows at moderate Reynolds number,  $Re_\tau = 300$ . A vortex detection method based on the imaginary part of the eigenvalue of the velocity gradient tensor has helped to identify the vortices in velocity fields. The vortex packet structure found in present study is consistent with and substantiates the observations and the results from previous 2-D PIV measurements. This evidence substantiates the view that vortex packets are a universal feature of wall turbulence, independent of effects due to boundary layer trips or critical conditions in the aforementioned numerical studies. Visualization of DNS velocity field and vortices also shows the close association of hairpin packets with long low-momentum streaks

## INTRODUCTION

Previously, Head and Banyopadyhay (1981) conducted flow visualization of boundary layer flows using smoke and a laser light sheet in a low speed wind tunnel. They observed that the boundary layer flow is full of hairpin vortices. The hairpin vortices found in their experiments arise from the wall and incline at 45 degrees with the hairpin heads aligned along a 20-degree line downstream. They suggested that groups of individual hairpin vortices are a major component of the turbulent boundary layer. Haidari and Smith (1994) performed experiments in a laminar boundary layer with an

impulsive fluid injection and observed the formation of a hairpin group also.

By examining the signatures left by coherent structures in the velocity fields, recent 2D PIV experiments have consistently revealed, that turbulent boundary layer (Meinhart & Adrian, 1995, 1999; Tomkins *et al*, 1998) and channel (Liu *et al*, 1996) flows are densely populated with hairpin vortices that form coherent hairpin vortex packets. Meinhart and Adrian in their 2-D PIV experiments found multiple zones of nearly uniform streamwise momentum suggesting that the boundary layer is made up of a hierarchy of hairpin vortex packets. The younger packets are located near the wall with older ones on top of them. Tomkins *et al* (1998) did measurements with 2-D wide angle PIV at high Reynolds number and observed the geometry of full vortex packets. These 2-D PIV experiments provide evidence that the hairpin packets are a frequent occurring coherent structure.

To understand the formation of coherent hairpin packets a direct numerical simulation in a low Reynolds number ( $Re_\tau = 180$ ) turbulent channel flow by Zhou, Adrian and Balachandar (1998, 1999) has been performed to study the evolution of a single hairpin vortex into a packet. An initial hairpin-like structure generated by stochastic estimation based on two-point correlation of velocities was put into a main turbulent flow and allowed to evolve. They found that when the strength of the initial structure was above a threshold, it developed and formed a primary hairpin, and subsequently generated secondary and tertiary hairpins and later a downstream hairpin, as shown in Figure 1. These hairpin vortices organize themselves into a coherent packet aligned in the streamwise direction. The importance of this work is the disclosure of the complete Navier-Stokes mechanisms for the generation of vortex packet. It generally supports the previous finding of Smith *et al* (1991).

Although the PIV experiments and DNS evolution study present convincing evidence of the existence of packets, no existing DNS studies have reported observations of hairpin

packets and very few DNS studies even provide observations of individual hairpin vortices, and some have concluded that hairpins do not exist at all. Why is that? Do hairpin packets really exist in DNS wall turbulence? This question needs a convincing answer. The present DNS of fully developed turbulent channel flows at moderate Reynolds number ( $Re_\tau = 300$ ) has been performed with no initial structure added to the flow and no trips in the channel. The packets with mostly asymmetric hairpin vortices have been observed in both halves of the channel flow for every realization of the present simulation. They are the frequently occurring large-scale structure in both space and time. The observations are found to be consistent with previous 2-D PIV experiments of boundary layer and channel flows and the DNS evolution study. The 3-D capability of DNS data provides 3-D information for the packet structure and characteristics and a clearer picture than the 2-D visualizations. The present DNS study also observes a close association of packets with Q2 and Q4 events, long low-momentum streaks and the generation to Reynolds stress.

### DNS DATA OF CHANNEL FLOW

The DNS data of fully developed channel flows at moderate Reynolds number in the present study were generated by solving the full three-dimensional time-dependent Navier-Stokes equations using the pseudo-spectral code, originally developed by Lyons *et al* (1991). The Reynolds number,  $Re_\tau$ , based on the half channel height,  $h$ , and the friction velocity,  $u_\tau = \sqrt{\nu \partial U / \partial y|_{wall}}$ , is 300, where  $\nu$  is the kinematic viscosity and  $U(y)$  is the ensemble-mean streamwise velocity profile. Periodic boundary conditions were imposed in the streamwise and spanwise directions, and no-slip and no-penetration conditions held at both walls. The pseudo-spectral method uses Fourier series expansions in the streamwise ( $x$ ) and spanwise ( $z$ ) directions and Chebyshev polynomial series expansions in the wall-normal ( $y$ ) direction. The spatial derivatives of the velocity field were computed in spectral space. The algorithm made use of a time-splitting technique that involves three fractional steps to compute the non-linear convective term, the pressure term and the viscous term of the Navier-Stokes equations. The details of the algorithm have been described in Lyons *et al* (1991).

The computational domain in streamwise, spanwise and wall-normal directions is  $3800^+ \times 1900^+ \times 600^+$  in wall units ( $\nu/u_\tau$ ) with grid numbers of  $256 \times 256 \times 129$ , giving approximately 8.5 million data points. The grid spacing in wall units was 14.9 and 7.49 in  $x$  and  $z$  and ranged from 0.09 ~ 7.36 in  $y$ . The ensemble averaged mean velocity profile, RMS of the turbulent velocity fluctuations and the Reynolds stress profile obtained from the DNS data are shown in Figure 2. For comparison LDV data obtained from channel flow experiments at about the same Reynolds number (Guenther *et al*, 1998) are plotted together. Good agreements are shown in the figure.

### IDENTIFICATION OF HAIRPIN VORTEX PACKET

To identify vortices in an instantaneous 3D DNS flow field, a flow pattern analysis based on critical point concepts (Perry and Chong, 1987) is a very useful methodology. The

eigenvalues of the velocity gradient tensor of incompressible flow for every grid point in the flow field are obtained by solving the characteristic equation,  $\lambda^3 + Q\lambda + R = 0$ , where  $Q$  and  $R$  are the tensor invariants that determine the local flow pattern. The discriminant is  $D = (27/4)R^2 + Q^3$ . For  $D \leq 0$  eigenvalues are real. For  $D > 0$  there are one real and two complex conjugate eigenvalues for the tensor. In this case the flow pattern exhibits stable focus/stretching ( $R < 0$ ) or unstable focus/compressing ( $R > 0$ ). Zhou *et al* (1998, 1999) have identified the imaginary part of the complex conjugate eigenvalue,  $\lambda_{ci}$ , as a new kinematic quantity which they call the “swirling strength”. They used the swirling strength to identify vortices in their DNS evolution work. The identification of vortex using this technique is frame independent. The use of swirling strength has the additional advantage of avoiding regions of shearing motions with no swirling but strong vorticity. The present study, therefore, has adopted swirling strength as a means to identify vortices in DNS velocity fields.

### HAIRPIN VORTEX PACKETS IN DNS FLOW FIELD

To visualize the vortex packets, the velocity gradient tensor of the flow field for each grid point was computed spectrally, and then the imaginary part of its eigenvalue of was calculated. The iso-surfaces of vorticity  $|\omega|$  in Fig. 3a and the swirling strength  $\lambda_c$  in Fig. 3b are shown in a small sub-domain of  $1/16$  of the horizontal dimensions,  $950^+ \times 475^+$ , and a half of the channel height,  $300^+$ . The size of the sub-volume shown here is only  $1/32$  of the whole computation domain. From these figures, one can see that swirling strength captures vortices that contain concentrated vorticity but discards the shearing motions. In the view looking downstream from above, asymmetric hairpins with clear spanwise heads are seen apparently, and they are aligned in the streamwise direction. Such a hairpin group forms a packet with a length longer than 1000 wall units in the streamwise direction. In this sub-domain, as shown in Fig. 3b and 3c, three packets can be identified with a spanwise spacing of 150 ~ 200 wall units. Figure 3d is a side-view that shows hairpin legs and quasi-streamwise vortices extending along the wall and gradually tilting up downstream at an angle of 30 ~ 45 degrees. Some of them turn spanwise and connect the heads.

Fluctuating velocity fields obtained from the present numerical simulation are shown in Figure 4 with three cut-views in  $xy$ -,  $xz$ - and  $yz$ -planes. Signatures of hairpins and packets can be observed. Hairpin heads appear as spanwise vortices in the  $xy$ -plane (Fig. 4a) and form a line inclined with an angle of about 10 to 15 degrees with the wall. Below the heads a strong low-momentum flow appears as a result of collective pumping effect by the hairpin legs and heads in the packet. The low-momentum fluid meets the high momentum fluid from the outer region of the channel and forms stagnation points and a shear layer. This kind of inclined structure, as a signature left by the packet, occurs everywhere starting from the wall to the region of about 200 wall units high. It has a length of about 1000 ~ 2000 wall units in the streamwise direction, and sometimes reaches the center of the channel and beyond. Long low-momentum streaks created by the packets are observed in the  $xz$ -plane (as shown in Fig. 3b at  $y^+ = 10$ ) with a length of 1000 to 2000 wall units

the channel and beyond. Long low-momentum streaks created by the packets are observed in the  $xz$ -plane (as shown in Fig. 3b at  $y^+ = 10$ ) with a length of 1000 to 2000 wall units in streamwise direction. The spanwise spacing of neighboring streaks ranges from 100 to 200 wall units. Cross-sections of the tilted hairpin legs are observed as elliptical shaped vortices at flanks of the low-momentum streaks in the  $xz$ -plane and as circular shaped vortices in the  $yz$ -plane (Fig. 3c). The  $yz$ -plane cut-view also shows the low-momentum fluid being pumped up by the hairpin legs, the quasi-streamwise vortices, moving away from the wall region. Sometimes it goes beyond the channel center due to the pumping effects by the hairpin head.

Figure 5 is a side-view of a single hairpin packet comprising at least four hairpin vortices with their heads aligned in a line making an angle of 11 degrees with the wall in the streamwise direction, the similar angle seen in Fig. 4a. The younger hairpins in the packet are located upstream with smaller inclination to the wall, while the older ones are located downstream with larger tilting angles and grow more away from the wall. The spanwise width of this packet is found to be about 200 wall units. In the spanwise direction the older hairpin heads grow wider and the packet expand in an open angle of  $10 \sim 12$  degrees, as shown in Figure 6. The whole packet convects downstream as a coherent structure with little and slow dispersion. Figure 7 shows the packet convecting downstream in  $t = 0$  and  $t = 4$  viscous time units with no obvious change in shape. The convection velocity,  $u_c$ , is about  $12u_\tau$ , or 76% of the bulk velocity of the channel,  $u_b$ , for the particular packet.

As the packet grows the older hairpins in the packet develop further away from the wall, very often a new younger packet occur below them, as also shown by Tomkins *et al* (1998). In this manner, a hierarchy of packets forms with older packet on top of the younger ones. Figure 4a shows the hierarchy of packet involving at least three packets (marked by inclined lines) with the older one growing beyond the channel center and the younger ones occurring close to the wall having smaller inclining angles.

As a consequence of the sequence of hairpin vortices in the packet aligned one behind the other along the streamwise direction, a long low-momentum streak is created. These kind of long low-momentum streaks are obviously seen in Figures 4a and 4b. Each hairpin in the packet contributes part of the long streak. As a result the long streak appear twisted in a quasi-streamwise direction, as seen in the  $xz$ -plane cut-view in Fig. 4b. The length of the long streak is apparently longer than 1000 wall units. In the inboard of the hairpins the quasi-streamwise legs and also the hairpin heads pump low-momentum fluid away from the wall. Their collective actions of pumping form strong Q2 events. On the other hand, in the outboard sides of the legs and above the heads high momentum fluid is pumped downward from the outer region of the channel, and Q4 events occur. Consequently, these Q2 and Q4 events contribute strong Reynolds stress

## CONCLUSIONS

The present study presents results that provide clear evidence for the existence of hairpin packets in DNS channel flow. Although a few previous DNS studies showed the existence of hairpin vortices the present study, for the first

time, reveals the existence and the frequent occurrence of hairpin packets in DNS of wall turbulence

The present observations of the structure and the characteristics of the coherent packet are consistent with and substantiate the previous observations from 2-D PIV experiments by Meinhart & Adrian (1995, 1999) and Tomkins *et al* (1998) for boundary layer flows, and the evolution study in DNS channel flow by Zhou, Adrian and Balachandar (1999).

## ACKNOWLEDGMENTS

This work was supported by NSF and AFOSR. The support and computational facilities of National Center for Supercomputation Applications of the University of Illinois at Urbana-Champaign, Illinois, are gratefully acknowledged.

## REFERENCES

- Guenther A., Papavassiliou D. V., Warholic M. D., Hanratty T. J., 1998, "Turbulent flow in a channel at a low Reynolds numbers", *Exp. Fluids*, Vol. 25, pp.503-511.
- Hardari A. H. and Smith C. R., 1994, "The generation and regeneration of single hairpin vortices," *J. Fluid Mech.*, Vol. 175, pp. 135-162.
- Head M. R. and Bandyopadhyay P. B., 1981, "New aspects of turbulent boundary-layer structure," *J. Fluid Mech.*, Vol. 107, pp. 297-338.
- Liu Z. C., Adrian R. J., Hanratty T. J., 1996, "A study of streaky structure in a turbulent channel flow with particle image velocimetry", *8<sup>th</sup> Int. Symp. on Appl. of Laser Techn. to Fluid Mech.* Lisbon, pp. 17.1.1-17.1.9.
- Lyons S. L., Hanratty T. J. and McLaughlin J. B., 1991, "Large-scale computer simulation of fully developed turbulent channel flow with heat transfer," *Intl. J.Numer. Meth. in Fluids*, Vol. 13, pp. 999-1028.
- Meinhart C. D. and Adrian R. J., 1995, "On the existence of uniform momentum zones in a turbulent boundary layer," *Phys. Fluids*, Vol. 7, pp. 694-696.
- Meinhart C. D., Adrian R. J. and Tomkins C. D., 1999, "Vortex organization in the outer region a turbulent boundary layers," Manuscript in preparation.
- Perry A. E and Chong M. S., 1987, "A description of eddying motions and flow patterns using critical-point concepts," *Ann. Rev. Fluid Mech.*, Vol. 19, pp. 125-155.
- Smith C. R., Walker, J. D. A., Haidari, A. H., and Sobrun, U., 1991, "On the dynamics of near-wall turbulence," *Phil. Trans. of Roy. Soc. London A*, Vol. 336, pp. 131-175.
- Tomkins C. D., Adrian R. J. and Balachandar S., 1998, "The structure of vortex packets in wall turbulence," *AIAA* 98-2962, pp. 1-13.
- Zhou J., Meinhart C. D., and Balachandar S. and Adrian R. J., 1998, "Formation of coherent hairpin packets in wall turbulence," *Self-Sustaining Mechanisms of Wall Turbulence*, Chapter 6. Editor: Panton R. L., pp. 109-134.
- Zhou J., Adrian R. J., Balachandar S. and Kendall T. M., 1999, "Mechanisms for generating coherent packets of hairpin vortices in near-wall turbulence," *J. Fluid Mech.*, Vol. 387, pp. 353-396.

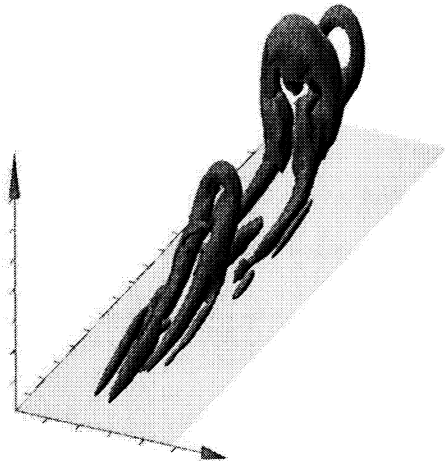
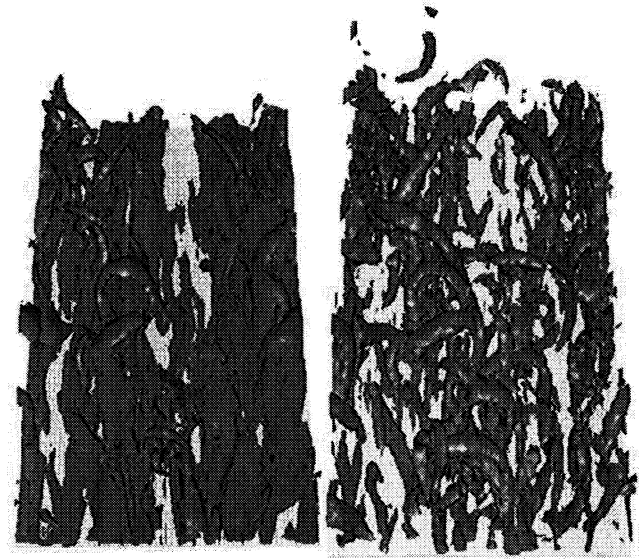


Figure 1. Hairpin vortex packet evolved from an initial single hairpin (Courtesy from Zhou et al, 1999)



(a)

(b)

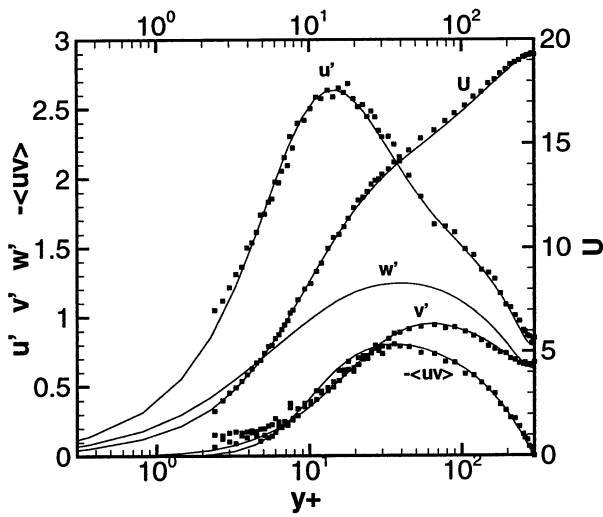


Figure 2. Mean velocity profile, RMS of turbulent velocity fluctuations and Reynolds stress profile, with LDV data points (dots) plotted for comparison.



(c)



(d)

Figure 3. Iso-surfaces of vorticity (a), and swirling strength (b), (c) and (d) in a top-view, an end-view and a side-view of a sub-volume of  $\Delta x = 950$ ,  $\Delta y = 300$  and  $\Delta z = 475$  wall units.

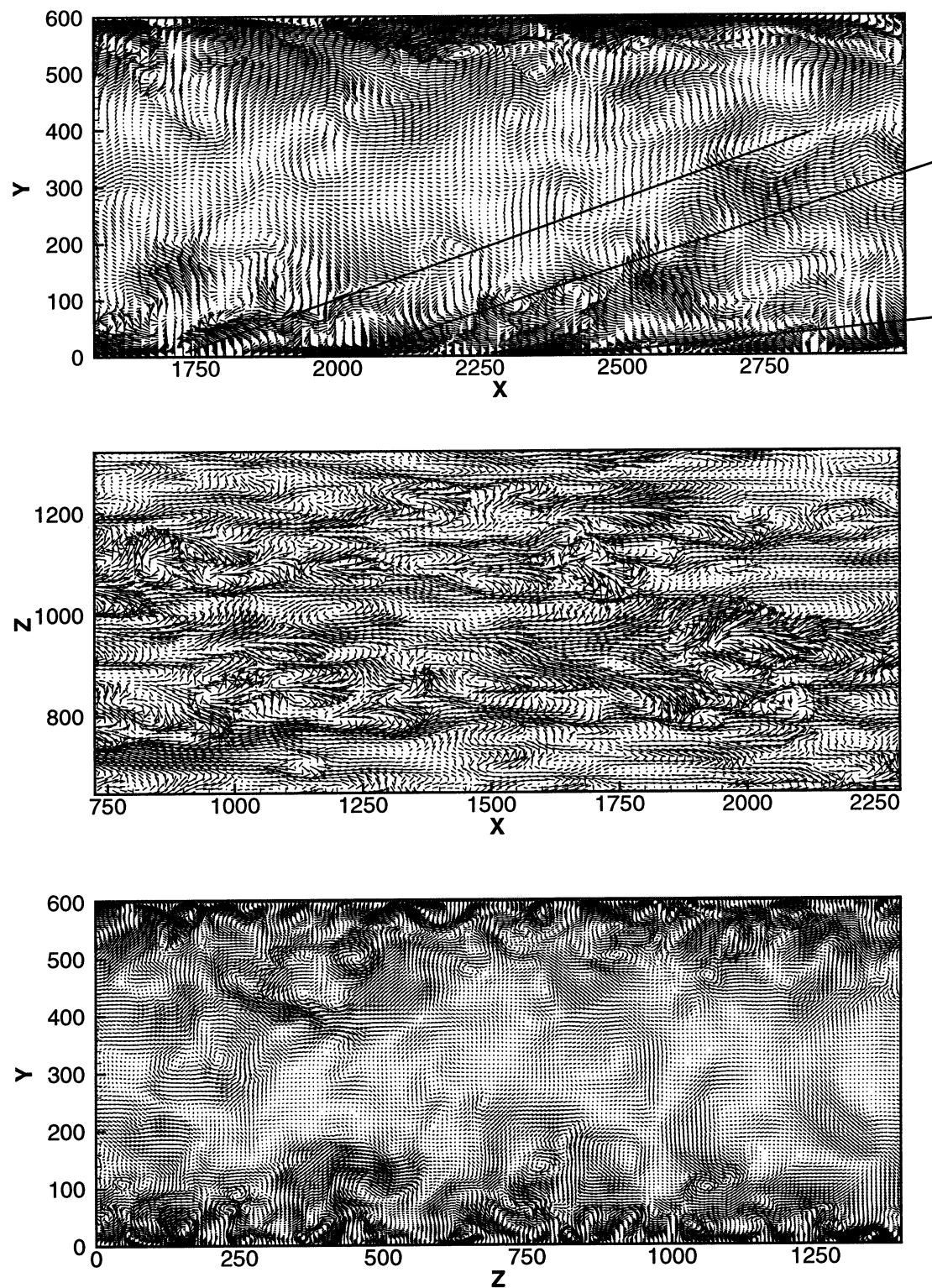


Fig 4. Instantaneous DNS fluctuating velocity fields at  $Re_\tau = 300$ . Upper: an xy-plane cut-view. Middle: an xz-plane cut-view. Bottom: a yz-plane cut-view. All coordinates are in wall units.

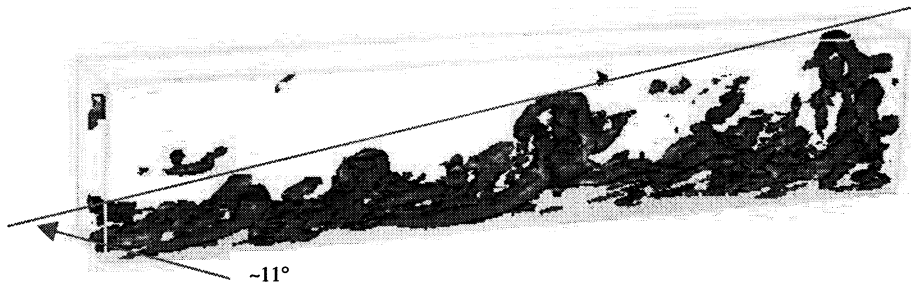


Figure 5. A single hairpin packet in a sub-domain of  $\Delta x = 950$ ,  $\Delta y = 300$  and  $\Delta z = 150$  wall units.

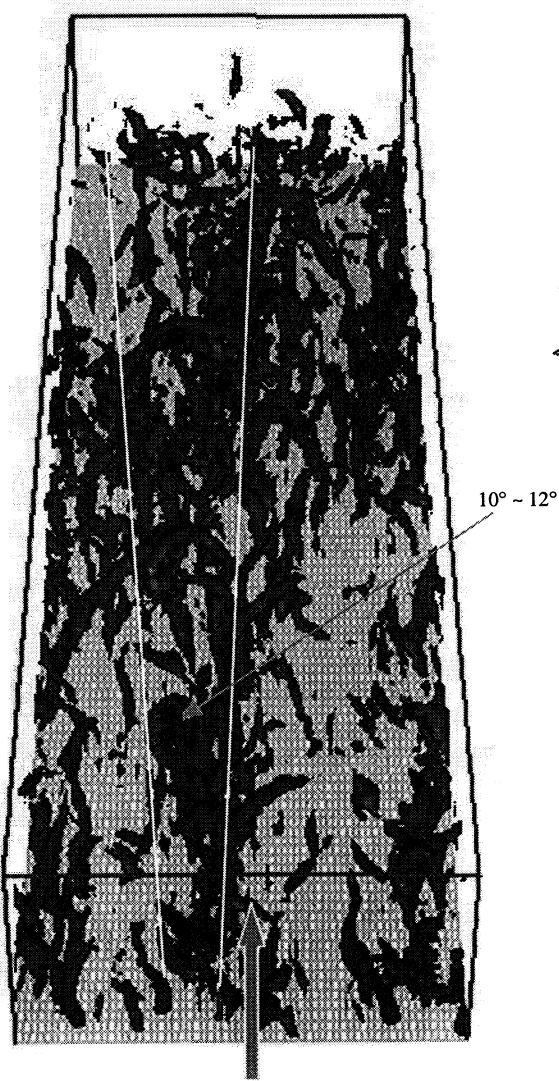


Figure 6. A top view of a packet. Sub-domain:  $\Delta x = 1200$ ,  $\Delta y = 264$  and  $\Delta z = 475$  wall units.

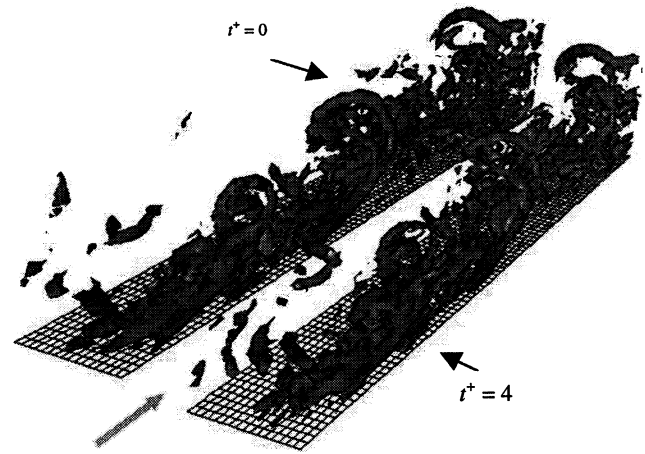


Figure 7. Packet in two time steps with 4 viscous time units apart. It convects downstream with velocity  $u_c = 12 u_\tau = 0.76 u_b$ . Sub-domain:  $\Delta x = 1200$ ,  $\Delta y = 264$  and  $\Delta z = 200$  wall units.